

## Supplemental Methods

### Mass spectrometry and data analysis

Samples were first loaded and desalted on a trap (0.1 mm id x 20 mm) at 10  $\mu$ L/min with 0.1% formic acid for 15 min and then separated on an analytical column (75  $\mu$ m id x 25 cm) (both PepMap C18) over a 60 min linear gradient of 4%–33.6% CH<sub>3</sub>CN/0.1% formic acid at 300 nL/min and total cycle at 90 min. The LTQ FT was operated in standard top 5 data-dependent acquisition. The survey scans (m/z 380-1800) were acquired on the FT-ICR at a resolution of 100,000 at m/z 400. The 5 most abundant multiply charged ions with a minimal intensity of 1000 counts were subject to MS/MS in the linear ion trap at an isolation width of 2 Th. Dynamic exclusion width was set at  $\pm$  1.5 Da for 60 s. The automatic gain control target value was regulated at 5E5 for FT and 8000 for the ion trap, with maximum injection time at 500 ms for FT and 200 ms for the ion trap, respectively.

The raw files were processed with Proteome Discoverer v1.4 (Thermo Fisher Scientific). Database searches were performed with Mascot 2.5 (Matrix Science) against the human Uniprot database (2014, 77606 entries) and an in-house contaminant database. The search parameters were: trypsin/P digestion, 2 missed cleavages, 10 ppm mass tolerance for MS, 0.5 Da mass tolerance for MS/MS, with variable modifications of acetyl (N-terminal), carbamidomethyl (C), N-formylation (protein), oxidation (M), and pyro-glu (N-term Q). Database search results were refined through processing with Percolator (FDR < 1%). Protein identification required at least one high-confidence peptide (FDR < 1%) with a minimum score of 20.

External contaminants (keratins, albumin, casein, trypsin, TEV protease, calmodulin) were removed from protein lists. For discrimination of high confidence true NBEAL2-associated proteins, protein hits identified in control samples by up to one third of unique sequences compared to target were not further considered.

### **Immunoprecipitation of endogenous proteins**

Protein complexes were eluted by suspending the beads in 1xLDS Sample Buffer (NP0007, Invitrogen). Samples were heated at 70°C for 10 min and loaded onto SDS-PAGE.

### **Proximity Ligation Assays**

Human megakaryocytes were generated from CD34<sup>+</sup> cells isolated by magnetic cell sorting and cultivated in CellgroSCGM in the presence of TPO (100 ng/mL) and IL1 $\beta$  (10 ng/mL). Megakaryocytes were harvested at day 10 and allowed to attach to fibrinogen-coated coverslips for 3 hours at 37°C. Cells were fixed with 2% formaldehyde-PBS for 30 min, washed with PBS and the assay was carried out following manufacturer's protocol. Primary antibodies used were Goat-anti Nbeal2 (SC243582 from Santa Cruz Biotechnologies, Heidelberg, Germany), rabbit anti-Sec16a (ab70722, Abcam, Cambridge, UK), rabbit anti-Vac14 (ab117940, Abcam), rabbit anti-Dock7 (ab118790, Abcam), mouse anti-CD42a (BD55816, BD Pharmingen), rabbit anti-CD42b (SC292722, Santa Cruz Biotech), mouse anti-CD41 (CD41UL-100, alphadiagnostic), and respective rabbit (I8140, Sigma), goat (SC2028, Santa Cruz Biotech) and mouse (M5409, Sigma) isotype controls. Phalloidin-488 was used to counterstain the cells (49409, Sigma).

Images were acquired using a Leica Sp5 inverted confocal microscope with the 63x immersion-oil objective and the Leica LAS 2.1 software. Maximum-intensity projections of the whole stacks were then prepared and color merge was applied for simultaneous visualization of different channels.

### **Isolation of platelets**

Platelet-Rich Plasma (PRP) was obtained and platelets were washed twice in Tyrode's buffer (137 mM NaCl, 2.9 mM KCl, 12 mM NaHCO<sub>3</sub>, 0.42 mM Na<sub>2</sub>HPO<sub>4</sub>, 2 mM MgCl<sub>2</sub>, 10 mM HEPES, 5.5 mM glucose), pH 6.5. Finally, platelets were resuspended in Tyrode's buffer pH 7.35 containing 1mM CaCl<sub>2</sub>. The platelet count was adjusted according to the experiment to carry out.

### **Immunoblots**

Supernatants were obtained and a Bradford assay was performed to measure protein concentration. Samples were resolved on 4-12% Bis-Tris Nupage gels and semi-dry transfer. Densitometry was performed using ImageStudio.

For the study of phospho-proteins, three volumes of platelets were lysed with one volume of 4xLDS Sample Buffer.

### **F-actin formation in platelets**

Washed platelets at  $3 \times 10^5$  platelets/uL were activated with 0.5 u/mL thrombin for 10 min and then fixed, permeabilized and incubated with 488-Phalloidin (49409, Sigma) for 20 min. Samples were further diluted in PBS and read in a Gallios flow cytometer (Beckman Coulter, UK).

### **Platelet spreading on Fibrinogen**

Coverslips were washed twice with PBS and blocked with 1% BSA. Platelets at  $5 \times 10^3$  platelets/ $\mu\text{L}$  in Tyrode's buffer pH 7.35 were seeded onto the coverslips and platelet agonists or vehicle were added, i.e. 0.01 and 0.5 U/mL thrombin, 1  $\mu\text{g}/\text{mL}$  collagen-related peptide (CRP, Farndale Group, Department of Biochemistry, Cambridge University); and 10  $\mu\text{M}$  ADP (A2754, Sigma). Wells were then washed with PBS after 20 min at 37°C, and platelets fixed with 2% formaldehyde for 30 min. Staining was performed as described below. A Leica Sp5 inverted confocal microscope was used to acquire images.

### **Transmission electron microscopy and gold-labeling**

For CHRF:

After fixation, samples were washed five times in 0.1M HEPES and treated with 1% osmium ferricyanide at RT for 2 hours. Samples were rinsed 5 times in deionized-water and treated with 2% uranyl acetate in 0.05M maleate buffer pH 5.5 for 2 hours at RT, followed by a further wash in deionized-water and dehydration in an ascending series of ethanol solutions from 70% to 100%, followed by treatment with 2 changes of dry acetonitrile and infiltration with Quetol epoxy resin. Sections were cut at 50 nm on a Leica Ultracut S, stained with uranyl acetate and lead citrate and viewed at 120kV in an FEI Tecnai G2 TEM. Images were captured with an AMT XR60B camera using Deben software.

For gold-labeling, cells were washed as above but fixed in 8% formaldehyde-0.05M cacodylate solution, pH 7.4 overnight. Samples were rinsed in de-ionized water, stained in 2% uranyl acetate 0.05M maleate buffer pH 5.5, dehydrated to 100% dry ethanol, infiltrated with LR White resin for 2 days and this was

polymerised at 50°C for 48 hours. Thin sections were mounted on Nickel carbon film grids, incubated on drops of blocking buffer (Tris buffered saline containing 1% BSA, 0.1% Triton X100 and 0.1% Tween20) for 10 minutes. Grids were transferred to blocking buffer containing a mouse anti-FLAG antibody (1:25 dilution) at RT. They were rinsed (x8) in blocking buffer and incubated for 1 hour in blocking buffer containing an anti-mouse antibody conjugated to gold particles (1:100 dilution) for 1 hour at RT. They were rinsed as above and then washed (x4) in de-ionized water. Stained with 2% uranyl acetate in 50% ethanol and in Reynolds Lead Citrate. Sections were viewed in a Tecnai G2 as described above.

#### For platelets:

Platelets were prepared and labeled as previously described <sup>1</sup>. We used an “in-house” generated rabbit antiserum against a peptide spanning residues KVSTPPELLQEDQL of Nbeal2. This antiserum was used at a 1/50 dilution followed by an anti-rabbit antibody conjugated to gold particles of 10 nm of diameter.

#### **Confocal microscopy**

Samples were then incubated with ammonium chloride, permeabilized with 0.1% saponin-0.2% gelatin-PBS, and stained with the relevant primary and secondary antibodies prior to mounting. An anti-FLAG antibody was used to label PBW-FTAP. Tubulin and von Willebrand factor were also labeled with respective antibodies while actin filaments were labeled with Phalloidin-555 (SC363794, Santa Cruz Biotech). Secondary antibodies used were 488-goat anti-mouse IgG (F2761, Thermo Fisher Scientific, UK) and 555-conjugated goat anti-

rabbit IgG (A21428, Thermo Fisher Scientific). After incubation with antibodies, samples were washed in saponin-gelatin-PBS and mounted in DAPI-mounting medium. Images were acquired using a Leica Sp5 inverted confocal microscope.

### **Supplemental References**

1. Nurden P, Jandrot-Perrus M, Combrie R, et al. Severe deficiency of glycoprotein VI in a patient with gray platelet syndrome. *Blood*. 2004;104(1):107-114.

**Table S1. List of antibodies used in this study**

<b>Antibody</b>	<b>Cat number</b>	<b>Supplier</b>
FLAG	F1804	Sigma
SEC16A	ab70722	Abcam
VAC14	ab117940	Abcam
DOCK7	ab118790	Abcam
CD41	CD41UL-100	Alpha diagnostic
CD42a	55816	BD Pharmingen
CD42b	292722	Santa Cruz Biotech
GAPDH	2118	Cell Signaling
P-Cofilin	3313	Cell Signaling
Cofilin	5175	Cell Signaling
Chronophin	4686	Cell Signaling
IQGAP1	ab133490	Abcam
RAC1	05-389	Milipore
CDC42	05-542	Milipore
NBEAL2 (Rb)	ab187162	Abcam
NBEAL2 (Gt)	SC243582	Santa Cruz Biotech
TUBULIN-A1C	SC134239	Santa Cruz Biotech
vWF	A0082	Dako
Calreticulin	PA3-900	Thermo Fisher Scientific
$\beta$ -actin	ab8227	Abcam

**Table S2. The Nbeal2 interactome.**

Accession	Gene name	Description	Score	Coverage	Peptides	Peptide Spectrum Matches	Protein Class	Validation (Reverse IP)
Q9UKV8	AGO2	Protein argonaute-2	47.27	1.51	1	1	protein translation	
O00170	AIP	AH receptor-interacting protein	95.18	4.24	1	2	chaperones/heat shock prtoteins	
O43823	AKAP8	A-kinase anchor protein 8	61.59	6.21	2	2	enzymes/enzyme modulators	
Q9ULX6-2	AKAP8L	Isoform 2 of A-kinase anchor protein 8-like	64.43	2.56	2	2	enzymes/enzyme modulators	
P49419-2	ALDH7A1	Isoform 2 of Alpha-aminoadipic semialdehyde dehydrogenase	67.40	5.09	2	3	enzymes/enzyme modulators	
Q86V81	ALYREF	THO complex subunit 4	94.94	14.01	2	2	nucleic acid binding	
Q4VCS5-2	AMOT	Isoform 2 of Angiomotin	21.92	2.96	1	1	receptor activity/receptor activity	
Q9BQE5	APOL2	Apolipoprotein L2	38.08	3.26	1	1	receptor activity/receptor activity	
HOYH87	ATXN2	Ataxin-2 (Fragment)	743.02	19.65	17	34	receptor activity/receptor activity	Interaction not replicated
Q8WWM7-6	ATXN2L	Isoform 6 of Ataxin-2-like protein	215.40	13.33	9	16	nucleic acid binding	
O95816	BAG2	BAG family molecular chaperone regulator 2	263.04	41.23	10	13	chaperones/heat shock prtoteins	
O95429-2	BAG4	Isoform 2 of BAG family molecular chaperone regulator 4	78.72	6.65	2	2	chaperones/heat shock prtoteins	
B0UX83	BAG6	HLA-B associated transcript 3	66.45	4.26	3	3	chaperones/heat shock prtoteins	
HOYJB9	C14orf166	UPF0568 protein C14orf166 (Fragment)	77.34	12.40	1	1	protein dimerization	
D6RHX9	CAMK2A	Ca <sup>2+</sup> /calmodulin-dependent protein kinase type II subunit alpha (Fragment)	27.78	50.00	1	1	enzymes/enzyme modulators	
E9PLA9	CAPRIN1	Caprin-1 (Fragment)	38.71	22.04	2	2	nucleic acid binding	
E5RGU7	CCAR2	DBIRD complex subunit KIAA1967 (Fragment)	118.00	26.67	3	5	enzymes/enzyme modulators	
E5RHJ4	CCAR2	DBIRD complex subunit KIAA1967 (Fragment)	224.40	10.47	2	3	enzymes/enzyme modulators	
G3V119	CCAR2	DBIRD complex subunit KIAA1967	308.55	14.88	6	7	enzymes/enzyme modulators	
G5E9B2	CCT8	Chaperonin containing TCP1, subunit 8 (Theta), isoform CRA_a	1477.44	41.68	26	53	chaperones/heat shock prtoteins	
Q00587-2	CDC42EP1	Isoform 2 of Cdc42 effector protein 1	22.21	4.95	1	1	enzymes/enzyme modulators	
Q6P1J9	CDC73	Parafibromin	73.90	5.27	3	3	enzymes/enzyme modulators	
Q8IWX8	CHERP	Calcium homeostasis endoplasmic reticulum protein	21.91	1.31	1	1	ion channel binding	
HOYBG1	CPEB4	Cytoplasmic polyadenylation element-binding protein 4 (Fragment)	23.98	7.48	1	1	protein translation	
Q10570	CPSF1	Cleavage and polyadenylation specificity factor subunit 1	228.75	5.89	7	8	enzymes/enzyme modulators	
O95639	CPSF4	Cleavage and polyadenylation specificity factor subunit 4	80.16	10.04	2	2	nucleic acid binding	
J3QT54	CPSF7	Cleavage and polyadenylation-specificity factor subunit 7 (Fragment)	38.04	6.34	1	1	nucleic acid binding	
Q8IUI8-2	CRLF3	Isoform 2 of Cytokine receptor-like factor 3	68.90	5.48	1	1	protein dimerization	
G5E9L5	DDX17	DEAD (Asp-Glu-Ala-Asp) box polypeptide 17, isoform CRA_a	91.46	7.73	1	3	transcription factors/cofactors	
P31689	DNAJA1	DnaJ homolog subfamily A member 1	702.29	33.25	13	26	chaperones/heat shock prtoteins	
O60884	DNAJA2	DnaJ homolog subfamily A member 2	48.42	5.34	2	3	chaperones/heat shock prtoteins	
C9JB42	DNAJB6	DnaJ homolog subfamily B member 6 (Fragment)	81.16	19.70	1	1	chaperones/heat shock prtoteins	
K7ELJ8	DNAJC7	DnaJ homolog subfamily C member 7	114.42	27.74	4	4	chaperones/heat shock prtoteins	
HOY7L2	DOCK7	Dedicator of cytokinesis protein 7 (Fragment)	40.49	0.92	1	1	enzymes/enzyme modulators	Interaction confirmed
G5E9S1	EIF4G1	Eukaryotic translation initiation factor 4 gamma 1	83.27	2.78	3	4	protein translation	
B1AN89	EIF4G3	Eukaryotic translation initiation factor 4 gamma 3	21.75	1.59	1	1	protein translation	
B1AM48	ELAVL2	Embryonic lethal, abnormal vision, Drosophila)-like 2 (Hu antigen B) (Fragment)	82.70	16.40	3	3	nucleic acid binding	
H7C0T0	FAM120A	Constitutive coactivator of PPAR-gamma-like protein 1 (Fragment)	60.52	5.06	1	2	nucleic acid binding	

B4E363	FARSA	Phenylalanine--tRNA ligase alpha subunit	83.28	5.24	2	2	enzymes/enzyme modulators	
G3XAD6	FIP1L1	FIP1 like 1 (S. cerevisiae), isoform CRA_d	215.31	11.90	4	8	nucleic acid binding	
A8MQB8	FMR1	Fragile X mental retardation protein 1	79.71	3.78	2	6	protein dimerization	
I3L1Z2	FXR2	Fragile X mental retardation syndrome-related protein 2 (Fragment)	45.77	18.64	1	1	protein dimerization	
C9JW88	GIGYF2	ERQ amino acid-rich with GYF domain-containing protein 2 (Fragment)	48.91	22.06	1	1	nucleic acid binding	
B5MBZ5	GPN1	GPN-loop GTPase 1	23.50	4.42	1	1	enzymes/enzyme modulators	
Q5T7U1	GTF3C5	General transcription factor 3C polypeptide 5	119.37	13.57	5	5	nucleic acid binding	
E9PIQ7	HAX1	HCLS1-associated protein X-1	59.36	7.28	1	1	interleukin-1 binding	
J3QS41	HELZ	Probable helicase with zinc finger domain	230.78	5.25	8	12	enzymes/enzyme modulators	
Q13151	HNRNPA0	Heterogeneous nuclear ribonucleoprotein A0	102.34	5.90	2	3	enzymes/enzyme modulators	
E7EWI9	HNRNPA3	Heterogeneous nuclear ribonucleoprotein A3	228.75	11.49	3	4	nucleic acid binding	
P51991	HNRNPA3	Heterogeneous nuclear ribonucleoprotein A3	228.75	10.58	3	5	nucleic acid binding	
D6R9P3	HNRNPAB	Heterogeneous nuclear ribonucleoprotein A/B	62.24	5.00	1	1	transcription factors/cofactors	
D6RF44	HNRNPD	Heterogeneous nuclear ribonucleoprotein D0 (Fragment)	112.07	14.29	2	4	transcription factors/cofactors	
Q2L7G6	HNRNPR	Heterogeneous nuclear ribonucleoprotein R	251.21	11.60	6	12	nucleic acid binding	
F8VZJ4	HSPA1B	Heat shock 70 kDa protein 1A/1B	4168.71	35.92	25	164	chaperones/heat shock prtoteins	Interaction not replicated
C9J3N8	HSPB1	Heat shock protein beta-1	50.21	91.89	2	3	enzymes/enzyme modulators	
H0Y5W0	HUWE1	E3 ubiquitin-protein ligase HUWE1 (Fragment)	132.98	1.47	3	3	enzymes/enzyme modulators	
F8W930	IGF2BP2	Insulin-like growth factor 2 mRNA-binding protein 2	595.19	9.92	6	17	protein translation	
F8WD15	IGF2BP3	Insulin-like growth factor 2 mRNA-binding protein 3	32.78	12.35	1	2	protein translation	
G5E9M5	ILF3	Interleukin enhancer binding factor 3, 90kDa, isoform CRA_b	162.33	9.24	6	9	nucleic acid binding	
E5RH50	LARP1	La-related protein 1 (Fragment)	97.16	7.69	4	6	protein translation	
G5E976	LARP4	La ribonucleoprotein domain family, member 4, isoform CRA_h	225.55	13.48	6	8	nucleic acid binding	
H0Y4V9	LARP4B	La-related protein 4B (Fragment)	131.10	18.88	6	9	nucleic acid binding	
K7ELG9	LSM12	Protein LSM12 homolog	88.66	11.74	2	2	unclassified	
Q5JR04	MOV10	Mov10, Moloney leukemia virus 10, homolog (Mouse)	118.89	6.23	4	5	nucleic acid binding	
G3V3L6	MTHFD1	C-1-tetrahydrofolate synthase, cytoplasmic	68.99	2.21	1	1	enzymes/enzyme modulators	
H7C3Y7	NBEAL2	Neurobeachin-like protein 2 (Fragment)	13076.55	38.79	47	587	phospholipid binding	NA (Bait)
B5MCN7	NCOA1	Nuclear receptor coactivator 1	25.01	1.36	1	1	enzymes/enzyme modulators	
O75376-2	NCOR1	Isoform 2 of Nuclear receptor corepressor 1	42.86	0.56	1	1	transcription factors/cofactors	
Q15233	NONO	Non-POU domain-containing octamer-binding protein	305.38	28.24	15	16	transcription factors/cofactors	
Q9BSD7	NTPCR	Cancer-related nucleoside-triphosphatase	47.82	7.89	1	1	enzymes/enzyme modulators	
H3BV41	NUDT21	Cleavage and polyadenylation-specificity factor subunit 5 (Fragment)	31.86	11.27	1	1	enzymes/enzyme modulators	
Q7Z417	NUFIP2	Nuclear fragile X mental retardation-interacting protein 2	270.87	16.83	8	10	nucleic acid binding	Interaction not replicated
O15294	OGT	cetylglucosamine--peptide N-acetylglucosaminyltransferase 110 kDa	52.97	1.53	1	1	enzymes/enzyme modulators	
P11940	PABPC1	Polyadenylate-binding protein 1	5299.40	63.84	60	287	protein translation	
Q13310-2	PABPC4	Isoform 2 of Polyadenylate-binding protein 4	2976.46	47.54	35	140	nucleic acid binding	
Q86U42-2	PABPN1	Isoform 2 of Polyadenylate-binding protein 2	46.39	7.43	1	1	nucleic acid binding	
E9PDH4	PIKFYVE	1-phosphatidylinositol 3-phosphate 5-kinase (Fragment)	41.94	1.01	1	1	enzymes/enzyme modulators	
O15160-2	POLR1C	Isoform 2 of DNA-directed RNA polymerases I and III subunit RPAC1	58.08	2.92	1	1	enzymes/enzyme modulators	

C9J4M6	POLR2B	DNA-directed RNA polymerase	51.63	1.27	1	2	enzymes/enzyme modulators	
P19388	POLR2E	DNA-directed RNA polymerases I, II, and III subunit RPABC1	87.06	6.67	1	1	enzymes/enzyme modulators	
C9J1F6	PRRC2A	Protein PRRC2A	67.91	3.60	5	5	nucleic acid binding	
B7Z5E2	PSMC2	26S protease regulatory subunit 7	21.37	4.05	1	1	enzymes/enzyme modulators	
E9PR38	PUM1	Pumilio homolog 1	104.82	4.56	3	4	nucleic acid binding	
F5GYT7	QKI	Protein quaking	26.28	41.46	1	1	nucleic acid binding	
Q5QPM0	RALY	Protein, autoantigenic (HnRNP-associated with lethal yellow homolog (M	20.85	4.65	1	1	nucleic acid binding	
F8WBP7	RANBP2	Putative peptidyl-prolyl cis-trans isomerase	52.89	25.49	1	1	enzymes/enzyme modulators	
BOQYT6	RANGAP1	Ran GTPase activating protein 1 (Fragment)	41.92	37.84	1	1	enzymes/enzyme modulators	
E9PC52	RBBP7	Histone-binding protein RBBP7	54.46	3.13	1	1	nucleic acid binding	
Q96PK6	RBM14	RNA-binding protein 14	293.42	22.27	13	14	transcription factors/cofactors	
G3V1T9	RBM7	RNA binding motif protein 7, isoform CRA_a	48.43	6.85	1	1	nucleic acid binding	
E7EPF2	RBMS1	RNA-binding motif, single-stranded-interacting protein 1 (Fragment)	31.25	12.50	1	1	nucleic acid binding	
HOY6E7	RBMX	RNA-binding motif protein, X chromosome, N-terminally processed (Fragr	219.46	27.74	8	12	nucleic acid binding	
P40937	RFC5	Replication factor C subunit 5	46.59	4.71	1	1	enzymes/enzyme modulators	
P62906	RPL10A	60S ribosomal protein L10a	24.35	3.69	1	1	nucleic acid binding	
C9JXB8	RPL24	60S ribosomal protein L24	68.39	10.74	1	1	nucleic acid binding	
E9PSS0	RPS13	40S ribosomal protein S13 (Fragment)	29.73	8.62	1	1	nucleic acid binding	
Q5JR95	RPS8	40S ribosomal protein S8	102.45	27.13	4	4	nucleic acid binding	
Q9Y3I0	RTCB	tRNA-splicing ligase RtcB homolog	296.92	18.81	8	11	nucleic acid binding	
E7ETR0	RUVBL1	RuvB-like 1	31.22	3.81	1	2	enzymes/enzyme modulators	
Q9Y230	RUVBL2	RuvB-like 2	68.17	11.45	4	4	chaperones/heat shock prtoteins	
J3KNL6	SEC16A	Protein transport protein Sec16A	140.52	2.29	5	7	protein binding	Interaction confirmed
Q8NC51-4	SERBP1	Isoform 4 of Plasminogen activator inhibitor 1 RNA-binding protein	73.88	12.66	3	3	nucleic acid binding	
B4DPM9	SHMT1	Serine hydroxymethyltransferase	45.77	2.61	1	1	enzymes/enzyme modulators	
HOYKH2	SLTM	SAFB-like transcription modulator (Fragment)	50.86	11.00	1	1	nucleic acid binding	
HOYLA4	SORD	Sorbitol dehydrogenase	29.39	2.68	1	1	enzymes/enzyme modulators	
B7Z6X7	SRBD1	S1 RNA-binding domain-containing protein 1	90.76	3.89	2	2	nucleic acid binding	
Q5JW30	STAU1	Double-stranded RNA-binding protein Staufen homolog 1	118.75	6.07	2	2	enzymes/enzyme modulators	
G5EA18	STAU2	Double-stranded RNA-binding protein Staufen homolog 2	203.01	20.62	5	5	nucleic acid binding	
E7ETX7	SUGP2	SURP and G-patch domain-containing protein 2	116.97	1.39	1	2	nucleic acid binding	
B4DJ45	TARDBP	TAR DNA-binding protein 43	150.07	7.05	2	2	transcription factors/cofactors	
Q9Y2W1	THRAP3	Thyroid hormone receptor-associated protein 3	97.19	3.14	2	2	transcription factors/cofactors	
H3BTQ1	TNRC6A	Trinucleotide repeat-containing gene 6A protein (Fragment)	21.67	4.43	1	1	nucleic acid binding	
B1AKE8	TRO	Trophinin (Fragment)	31.01	7.84	1	1	protein binding	
G3V1U9	TUBA1A	Tubulin alpha-1A chain	2731.19	50.00	19	109	cytoskeletal proteins	Interaction not replicated
Q13748	TUBA3C	Tubulin alpha-3C/D chain	1771.80	35.11	15	63	cytoskeletal proteins	
F8VW92	TUBB	Tubulin beta chain	1359.11	43.91	22	62	cytoskeletal proteins	Interaction not replicated
Q13885	TUBB2A	Tubulin beta-2A chain	972.82	37.30	18	47	cytoskeletal proteins	
P04350	TUBB4A	Tubulin beta-4A chain	735.51	32.88	15	26	cytoskeletal proteins	

P68371	TUBB4B	Tubulin beta-4B chain	1080.89	42.92	22	49	cytoskeletal proteins	Interaction not replicated
Q9BUF5	TUBB6	Tubulin beta-6 chain	303.14	17.71	8	13	cytoskeletal proteins	
K7EKE5	TUBG1	Tubulin gamma-1 chain	29.83	15.56	2	2	cytoskeletal proteins	
HOY5H6	UBAP2L	Ubiquitin-associated protein 2-like (Fragment)	53.57	3.92	1	1	nucleic acid binding	
F5H265	UBC	Polyubiquitin-C (Fragment)	1301.67	96.64	12	82	enzymes/enzyme modulators	Interaction not replicated
E7EMW7	UBR5	E3 ubiquitin-protein ligase UBR5	131.59	1.40	3	3	enzymes/enzyme modulators	
F8W810	d protein OS	Uncharacterized protein	52.00	3.43	1	1	enzymes/enzyme modulators	
Q92900-2	UPF1	Isoform 2 of Regulator of nonsense transcripts 1	393.05	12.79	11	19	nucleic acid binding	
Q08AM6	VAC14	Protein VAC14 homolog	52.51	4.22	2	3	receptor activity/receptor activity	Interaction confirmed
P16989	YBX3	DNA-binding protein A	717.29	31.45	10	19	enzymes/enzyme modulators	
HOYIQ2	YLPM1	YLP motif-containing protein 1 (Fragment)	45.63	1.38	1	1	nucleic acid binding	
Q9Y5A9	YTHDF2	YTH domain family protein 2	31.02	1.90	1	1	nucleic acid binding	
Q7Z2W4-2	ZC3HAV1	Isoform 2 of Zinc finger CCCH-type antiviral protein 1	151.18	4.72	2	2	enzymes/enzyme modulators	
Q96KR1	ZFR	Zinc finger RNA-binding protein	96.69	2.89	2	2	nucleic acid binding	
Q5VUA4	ZNF318	Zinc finger protein 318	78.39	2.46	4	4	nucleic acid binding	
Q5BKZ1	ZNF326	DBIRD complex subunit ZNF326	166.24	10.65	4	5	enzymes/enzyme modulators	

**Table S3. Transcript levels of *Dock7*, *Sec16a* and *Vac14* in murine megakaryocytes derived *in vitro* from control and *Nbeal2*<sup>-/-</sup> mice<sup>1</sup>.**

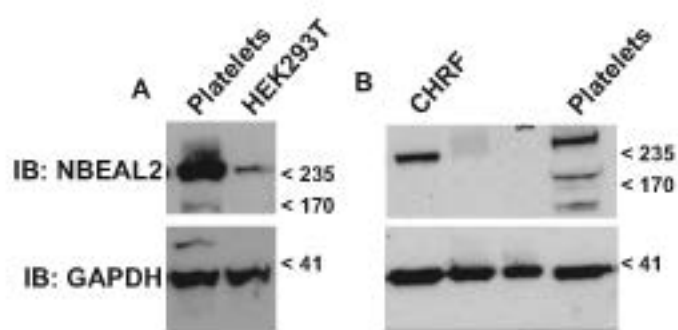
Probe ID	MGI.symbol	Control			<i>Nbeal2</i> <sup>-/-</sup>				P.Value	FDR
		Replicate 1	Replicate 2	Replicate 3	Replicate 1	Replicate 2	Replicate 3	Replicate 4		
ILMN_3890672	DOCK7	7.76	7.75	7.77	7.79	7.79	7.73	7.72	0.953727079	0.99611124
ILMN_870161	SEC16A	10.38	10.52	10.38	10.16	10.25	10.33	10.52	0.826461778	0.976975697
ILMN_4760291	VAC14	8.20	8.39	8.06	8.10	8.12	8.24	8.21	0.941924755	0.993776947

1. Guerrero JA, Bennett C, van der Weyden L, et al. Gray platelet syndrome: proinflammatory megakaryocytes and alpha-granule loss cause myelofibrosis and confer metastasis resistance in mice. *Blood*. 2014;124(24):3624-3635.

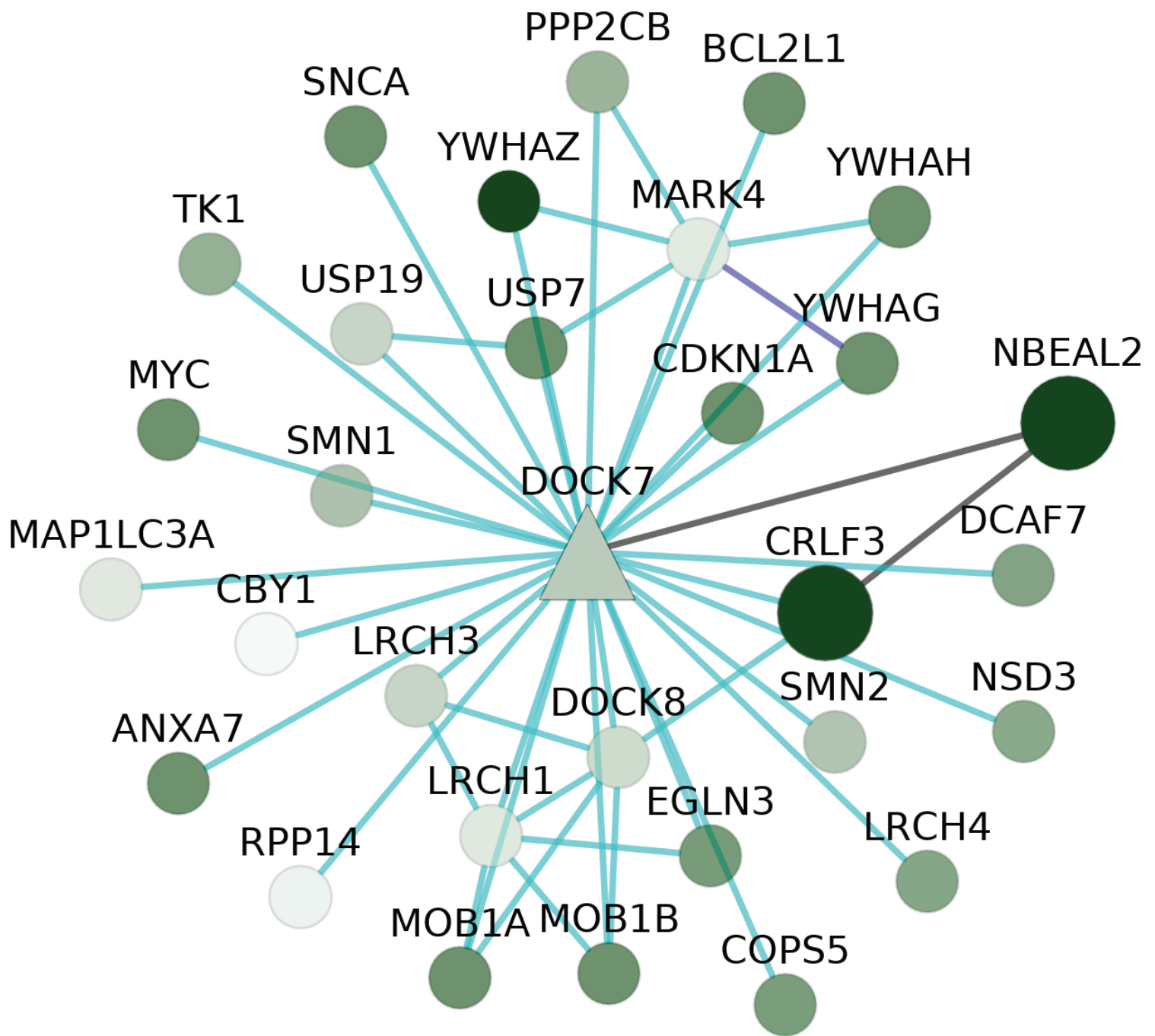
**Table S4. Transcript levels of *Iqgap1* in murine megakaryocytes derived *in vitro* from control and *Nbeal2*<sup>-/-</sup> mice<sup>1</sup>.**

		Control			<i>Nbeal2</i> <sup>-/-</sup>					
Probe ID	MGI.symbol	Replicate 1	Replicate 2	Replicate 3	Replicate 1	Replicate 2	Replicate 3	Replicate 4	P.Value	FDR
ILMN_3830377	IQGAP1	11.14	11.14	11.09	11.93	11.76	11.84	11.62	0.00007	0.06378

1. Guerrero JA, Bennett C, van der Weyden L, et al. Gray platelet syndrome: proinflammatory megakaryocytes and alpha-granule loss cause myelofibrosis and confer metastasis resistance in mice. *Blood*. 2014;124(24):3624-3635.



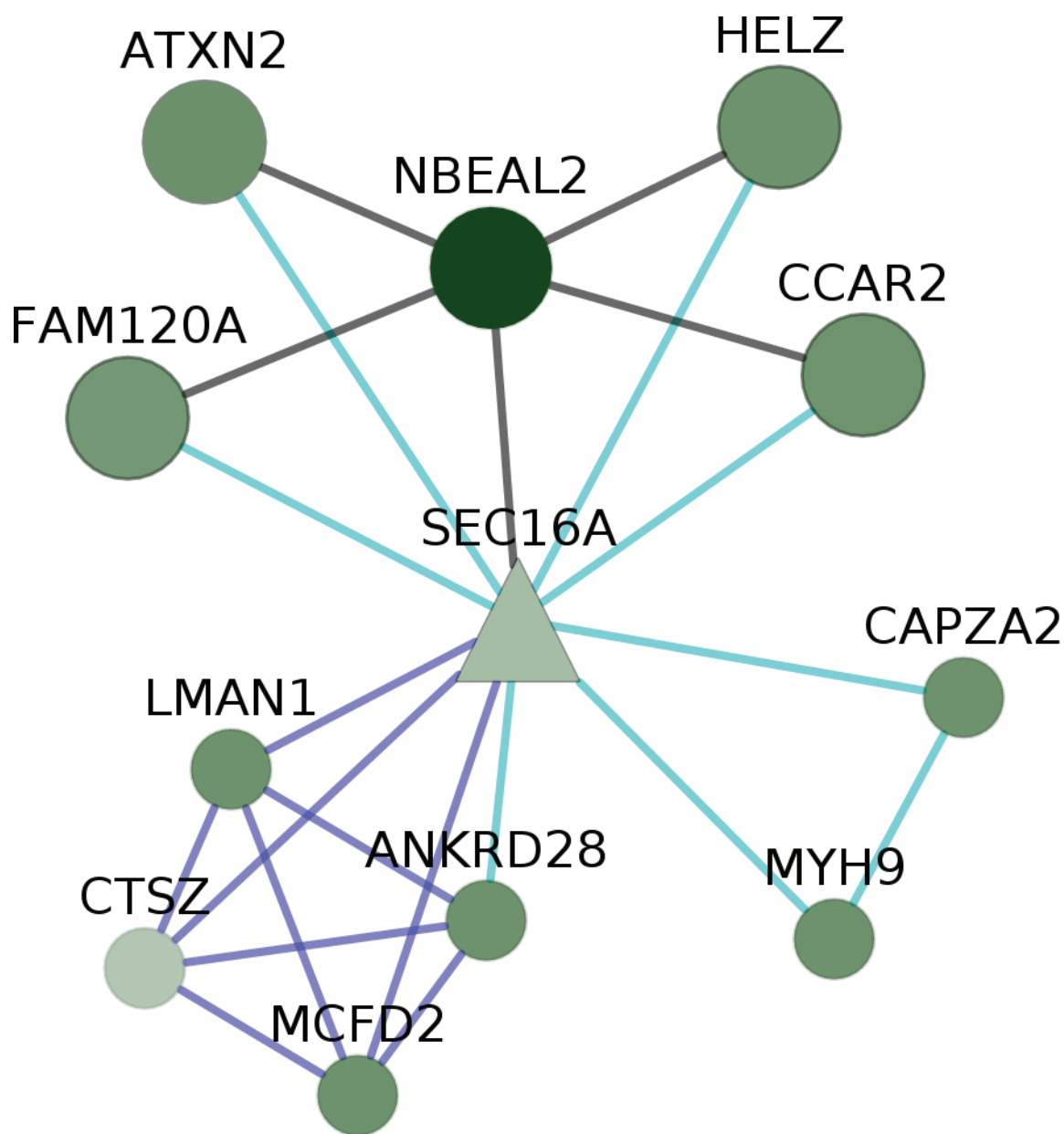
**Figure S1. Protein expression levels of Nbeal2 in the cell lines used in this study.** (A) Protein levels of Nbeal2 in HEK293T cells. (B) Protein levels of Nbeal2 in CHRF cells. Platelets were used for comparison and GAPDH used as loading control in A and B.



**Figure S2. Protein-protein interaction network (PPIN) of Dock7 and its first order interactors.** Reactome and IntAct databases were used to retrieve first order interactors of Dock7 shown as a triangle. Nodes corresponding to first order interactors of Dock7 whose transcript levels were below 1 fragment per kilobase of transcript per million mapped reads (FPKM) in human MKs are not depicted<sup>1</sup>. Color of nodes from white (lowest) to green (highest) indicates expression levels in FPKM. This PPIN contains 31 nodes and 46 edges. Interactions retrieved by IntAct and Reactome are shown as light and dark blue edges, respectively, while interactions from our Nbeal2 interactome are represented by black edges. Nodes corresponding to proteins present in the Nbeal2 interactome are larger.

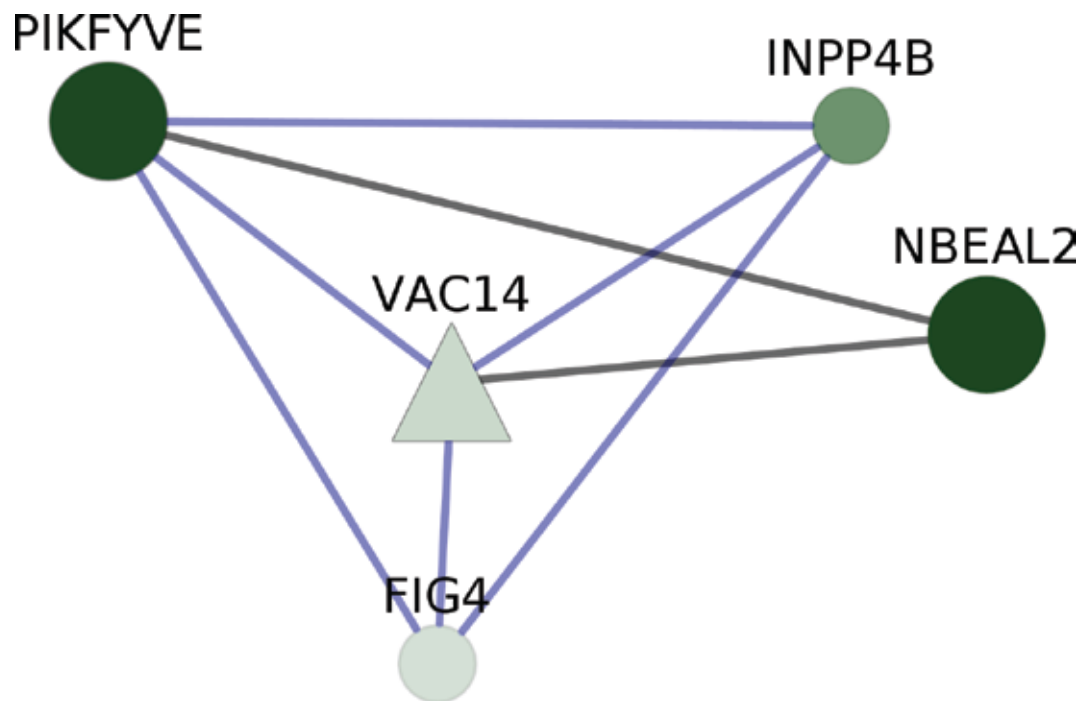
<sup>1</sup> Chen L, Kostadima M, Martens JHA, et al. Transcriptional diversity during lineage commitment of human blood progenitors. *Science*. 2014;345(6204):1251033.

Figure S3



**Figure S3. Protein-protein interaction network (PPIN) of Sec16a and its first order interactors.** Reactome and IntAct databases were used to retrieve first order interactors of Sec16a shown as a triangle. Nodes corresponding to first order interactors of Sec16a whose transcript levels were below 1 fragment per kilobase of transcript per million mapped reads (FPKM) in human MKs are not depicted<sup>1</sup>. Color of nodes from white (lowest) to green (highest) indicates expression levels in FPKM. This PPIN contains 12 nodes and 22 edges. Interactions retrieved by IntAct and Reactome are shown as light and dark blue edges, respectively, while interactions from our Nbeal2 interactome are represented by black edges. Nodes corresponding to proteins present in the Nbeal2 interactome are larger.

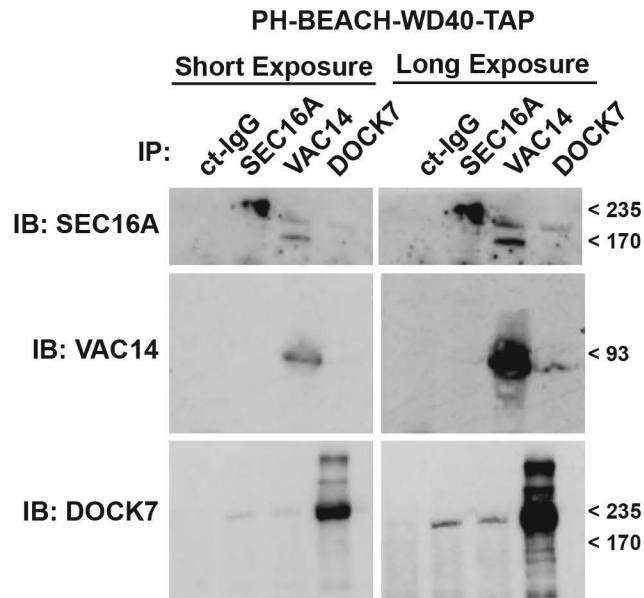
<sup>1</sup> Chen L, Kostadima M, Martens JHA, et al. Transcriptional diversity during lineage commitment of human blood progenitors. *Science*. 2014;345(6204):1251033.



**Figure S4. Protein-protein interaction network (PPIN) of Vac14 and its first order interactors.** Reactome and IntAct databases were used to retrieve first order interactors of Vac14 shown as a triangle. Nodes corresponding to first order interactors of Vac14 whose transcript levels were below 1 fragment per kilobase of transcript per million mapped reads (FPKM) in human MKs are not depicted<sup>1</sup>. Color of nodes from white (lowest) to green (highest) indicates expression levels in FPKM. This PPIN resulted in 5 nodes and 6 edges. Interactions retrieved by IntAct and Reactome are shown as light and dark blue edges, respectively, while interactions from our Nbeal2 interactome are represented by black edges. The black edges connecting Pikfyve with Fig4 and Vac14 were manually added. Nodes corresponding to proteins present in the Nbeal2 interactome are larger.

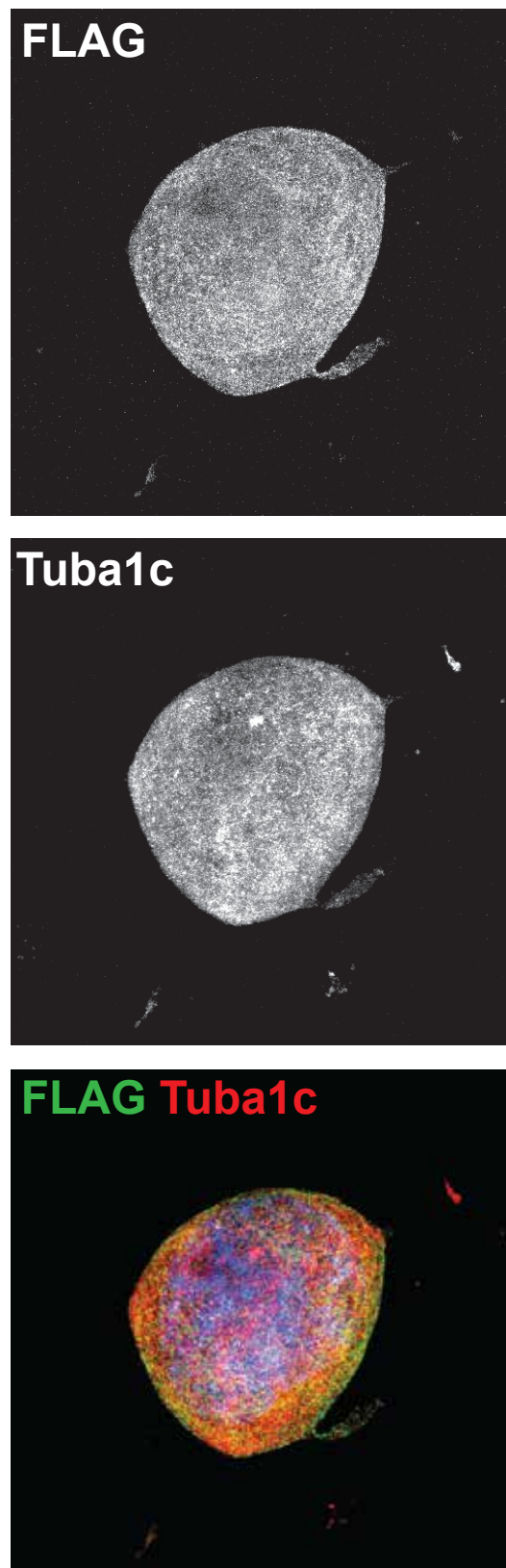
<sup>1</sup> Chen L, Kostadima M, Martens JHA, et al. Transcriptional diversity during lineage commitment of human blood progenitors. *Science*. 2014;345(6204):1251033.

Figure S5



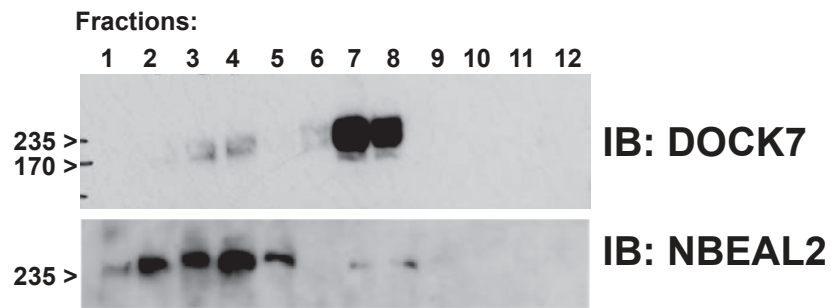
**Figure S5. Dock7, Sec16a and Vac14 interact with Nbeal2.** Immunoprecipitation of Dock7, Sec16a and Vac14 in PBW-FTAP HEK293T cells using specific antibodies and a control isotype as a negative control (short and long exposure times from original Figure 2B). Representative blots corresponding to short and long exposure of film to the chemiluminescence reagent developed with anti- Dock7, Sec16a and Vac14 antibodies. In addition to the captured bait in each lane, additional bands corresponding to one or two of the other interactors can be seen for each immunoprecipitation assay.

Figure S6



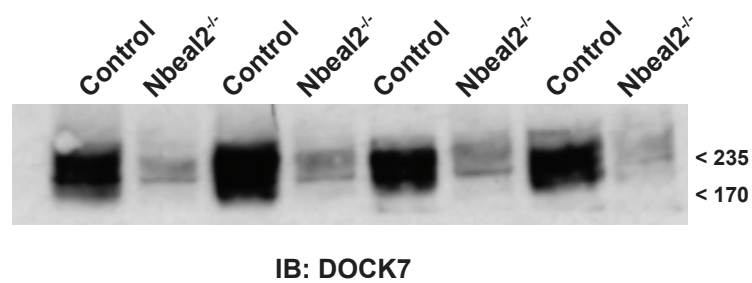
**Figure S6. Subcellular localization of PBW-FTAP in CHRF cells by confocal microscopy.** Labeling of PBW-FTAP and microtubules using anti-FLAG and anti-tubulin, respectively, visualized by confocal microscopy. Nucleus was stained with DAPI. Images are representative of three independent experiments.

Figure S7



**Figure S7. Subcellular localization of Nbeal2 and Dock7 in platelets.** Immunoblot analysis of Nbeal2 and Dock7 in mouse platelets after subcellular fractionation (extended from original Figure 5B and 5C). Longer exposure time (10 min) show that Nbeal2 and Dock7 partially colocalize in fractions 3, 4, 7 and 8.

Figure S8



**Figure S8. Dock 7 protein levels are reduced in platelets from Nbeal2<sup>-/-</sup> mice.** Western blot analysis of Dock7, in total platelet lysates from control and Nbeal2<sup>-/-</sup> mice (extended from original Figure 5F). Longer exposure to the chemiluminescence reagent indicates that Dock7 is still present in Nbeal2<sup>-/-</sup> platelets but its levels are significantly reduced as illustrated in Figure 5F (shorter exposure time and densitometry).